

ESTIMATION OF THE SOURCE TIME FUNCTIONS OF THE 1967 EGYPT EARTHQUAKE BY LOG-EXP FILTERING ON LONG PERIOD SEISMograms

KAILASH KHATTAR* AND RAJESH SHARMA**

Introduction

The mathematical modelling of earthquake sources has attained a considerable degree of refinement. Theoretical models are now available which satisfactorily describe the spatial and spectral (amplitude) radiation of elastodynamic fields from earthquakes (e.g., Ben-Menahem and Singh, 1972; Archambeau and Minster, 1977). Also many studies of the amplitude spectra recorded for earthquakes have led to a good understanding of this aspect of the energy radiation (Hanks and Wyss, 1972; Molnar et al., 1973; Wyss and Molnar, 1974). The study of the observed phase spectra of the earthquake sources has, however, failed to receive as much attention. Therefore, the determination of earthquake source time functions (e.g., the displacement time history as observed at a point near the fault in the elastic region) has not been as well studied as have been other source parameters, such as stress drop or slip. In a notable contribution, Dziewonski and Gilbert (1974) utilized normal modes to synthesize the temporal variation of the seismic moment tensor for two deep earthquakes. It is our purpose here to develop methods which facilitate the measurement of earthquake source time functions.

Under the stationary linear system model the seismograms available for such study are appropriately regarded as the convolved output of the wavelet representing the earthquake source time function with the transmission response of the earth-seismograph system. Therefore, in order to separate one signal from the convolved combination using conventional filtering techniques such as inverse Wiener filtering, the other signal must be known. The difficulty in separating the two components arises because, generally, the transmission response is not precisely known so the problem is essentially one of blind deconvolution. One approach to deconvolution that has been fairly successful in exploration seismology assumes the source to be minimum phase (Robinson, 1967). This assumption is not strictly applicable to a typical earthquake source time history, which will usually be a mixed phase signal. In spite of the above mentioned difficulties, some efforts have been made to estimate the source time histories of earthquakes. For example, Burdick and Helmberger (1974) extracted the source time functions of three deep focus events by deconvolving the transmission response which included the effects of instrument, crust, and anelastic attenuation in the earth.

Another approach for filtering convolved and multiplied signals is generalized linear, or homomorphic filtering (Oppenheim et al., 1968). The basic concept is that a product of signals can be mapped into an addition of signals by an appropriate transformation. In the transform domain the powerful techniques of linear filtering can then be utilized to separate

*Department of Earth Sciences, University of Roorkee, Roorkee. 247672 U.P.

**Institute of Reservoir Studies, Oil & Natural Gas Commission, Ahmedabad. 380003 Gujarat.

the desired components. This will, of course, be possible only if the signals in the transform domain are approximately not overlapping. Referring to the Fourier transform of an earthquake seismogram, we note that the earthquake source spectrum and the transmission-response spectrum are multiplied signals in the frequency domain. Therefore, the complex natural logarithm is the appropriate separator transform for our objective of converting the product into a sum. We assume the earthquake source spectrum to vary slowly with frequency, whereas the contribution from the transmission response tends to vary relatively more rapidly with frequency in the pass band of WWSSN long period seismographs. Consequently, in the inverse transform of the log of the complex spectrum of the seismogram we expect the contribution due to the earthquake source to occur near the origin, while that due to the earth transmission response to occur away from the origin. Thus, to recover the source time function we retain those values in the inverse transform that are near the origin. We have called this nonlinear filtering process LOG-EXP filtering. We note that Ulrych (1974) showed that the transmission response can be separated from the input source wavelet in this way. Also, Ulrych et al. (1972) and Clayton and Wiggins (1976) were able to extract the ground displacement pulse from earthquake seismograms using homomorphic deconvolution.

The objective of the present study is to analyze long period WWSSN seismograms using LOG-EXP filtering to extract the 1967 Koyna earthquake source time function and the earth transmission responses to the recording stations used in the analysis. The emphasis of the analysis, however, is on the recovery of the source time function.

Mathematical Preliminaries

A digitized earthquake seismogram $r(kt)$, which we shall henceforth write as r_k , may be represented by a convolution as follows:

$$r_k = s_k * g_k + n_k \quad (1)$$

where T denotes the sampling interval, which we will take as unity without loss of generality, s_k the source time function, g_k the earth-seismograph transmission impulse response, and n_k the additive noise. Assuming the noise to be negligibly small, the Z -transform of r_k is given by

$$R(Z) = \sum_{k=0}^{N-1} r_k Z^{-k} = S(Z) \cdot G(Z) \quad (2)$$

where $S(Z)$ and $G(Z)$ are the Z -transform of s_k and g_k , respectively, and N is the data length. Hence, taking the natural logarithm followed by an inverse Z transformation would convert the multiplication in (2) into an addition of signals.

$$\tilde{R}(Z) = \ln S(Z) + \ln G(Z)$$

or

$$\tilde{R}(Z) = \ln R(Z) = \ln |R(Z)| + j \arg R(Z)$$

and taking the inverse Z transform of $\tilde{R}(Z)$ we have

$$\hat{r}_l = \frac{1}{2\pi i} \oint_C \hat{R}(Z) Z^{l-1} dZ = \hat{s}_l + \hat{q}_l \quad (4)$$

where $l = 0, \pm 1, \pm 2, \dots$, and contour integration is counterclockwise.

The function \hat{r}_l , \hat{s}_l , and \hat{q}_l are the new functions corresponding to r_k , s_k , and q_k in the original time domain and are known as complex cepstrums (Schafer, 1969). The term 'complex' does not imply that the functions are complex; in fact they are real. It only signifies that phase information has also been used in deriving the functions. The independent variable l is called quefrency and has the dimensions of time. The terms cepstrum and quefrency are anagrams and are formed by reversing the first four letters of spectrum and frequency, respectively (Bogert et al., 1963; Schafer, 1969).

The inverse process to go back into the original time domain is defined by the following steps.

$$\begin{aligned} \hat{R}(Z) &= \sum_{l=-N/2+1}^{N/2} \hat{r}_l Z^{-l} \\ R(Z) &= \exp[\hat{R}(Z)] \\ r_k &= \frac{1}{2\pi i} \oint_C R(Z) Z^{k-1} dZ \end{aligned} \quad (5)$$

In practice the contour C is taken to be the unit circle and the fast Fourier transform algorithm is used for implementing the above procedure.

An analysis of the signal in the quefrency domain can also be done in a fashion analogous to the standard power spectral analysis. In this case only the cosine transform of $|R|$ is performed to give the power cepstrum.

Properties of the Cepstrum

The complex cepstrum has several important properties. Of particular interest in signal processing are the following (Schafer, 1969; Kemerait and Childers, 1972):

- 1) The complex cepstrum factors a signal into its maximum and minimum phase components. Let x_k be a mixed phase signal

$$x_k = x_k^{\text{min}} + x_k^{\text{max}} \quad (6)$$

Then in the quefrency domain we have

$$\hat{x}_l = \hat{x}_l^{\text{min}} + \hat{x}_l^{\text{max}} \quad (7)$$

such that

$$x_l^{\min} = 0 \text{ for } l < 0$$

$$x_l^{\max} = 0 \text{ for } l > 0$$

- 2) Another important property concerns repeated signals. Let

$$s_K = f_K + a f_{K-K_0} \quad (9)$$

where the signal consists of the original signal and its echo. Then the Z transform of s_K evaluated on the unit circle is

$$s(\omega) = F(\omega) [1 + ae^{-j\omega K_0}] \quad (10)$$

where the echo contributes a periodic component with period $2\pi/K_0$. This contribution becomes additive in the log spectrum.

$$\ln s(\omega) = \ln F(\omega) + \ln (1 + a e^{-j\omega K_0}) \quad (11)$$

Expanding the second term in a power series and evaluating the complex cepstrum gives

$$\hat{s}_l = \hat{f}_l + a \delta(l - K_0) - (a^2/2) \delta(l - 2K_0) + \dots \quad (12)$$

for $a < 1$, and

$$\hat{s}_l = a \hat{f}_{l-K_0} + (1/a) \delta(l + K_0) - (1/2a^2) \delta(l + 2K_0) + \dots \quad (13)$$

for $a > 1$. This illustrates the first property as well as the property that enables detection of an echo. The complex cepstrum will have spikes at frequencies corresponding to the echo time delay and its multiples. Similarly the power cepstrum will contain impulses at frequencies corresponding to the echo arrival time with magnitudes proportional to the magnitude of the echo.

A more general result can be derived for the model of a series of impulses representing the transmission response of a medium

$$s_K = \sum_{k=1}^N a_k \delta(t - K) \quad (14)$$

where a_K is the strength of the K -th arrival at time K . The Fourier transform of the impulse response is given by

$$I(\omega) = \sum_{k=1}^N a_k e^{-jk\omega} \quad (15)$$

and the log spectrum by

$$\begin{aligned} \hat{R}(z) = & \frac{1}{N} \ln \left[\sum_{K=1}^N a_K^2 + 2 \sum_{K=1}^N \sum_{J=1}^N a_K a_J \cos(\omega(K-J)) \right] \\ & + j \operatorname{Arctan} \left[\left(\sum_{K=1}^N a_K \sin \omega K \right) / \left(\sum_{K=1}^N a_K \cos \omega K \right) \right] \end{aligned} \quad (16)$$

Thus, for multiple echoes in the complex cepstrum $\hat{R}(z)$, we will find contributions at various combinations of the differences of arrival times. The magnitude of these contributions is likely to be almost always small in the case of the real earth as they represent products of small quantities (reflection coefficients).

In order to consider the effect of attenuation on complex cepstrum of echoes, let us consider that the spectrum of the echo is modified by a factor $e^{-\alpha z}$ as compared to the spectrum of the original signal due to the additional travel path. In this case the complex cepstrum given by (12) or (13) would have time functions of the form $\frac{2\alpha}{\alpha^2 + (L \pm nK_0)^2}$ instead of impulses corresponding to the contribution of the echo at $l=L$. Therefore, the complex cepstrum will appear smeared and it may not always be possible to identify the presence of echoes.

Results and Discussion

LOG-EXP analysis was done on three teleseismic recordings at WWSSN stations AAE, MAT (P-wave), and VAL (S-wave) for the 1967 Koyna Dam earthquake (hypocentral parameters determined by the India Meteorological Department are: Date December 10, 1967, Lat $17^{\circ}22.4'N$, Long $73^{\circ}44.8'E$, $M=6.3$, $H=8$ km, OT=22h 51m 19s). A long data window was selected in order to include the reverberations generated by the onset of the wave. The seismograms are shown in Figure 1. The seismograms were sampled at 0.5 sec intervals corresponding to the Nyquist frequency of 1 Hz. Computational considerations require that the sampling rate of the phase spectrum be rapid enough so that the computed phase in equation (16) (second term on the right side) is continuous (Schafer, 1969). The phase term usually has discontinuities because of the multivalued nature of the inverse tangent which can be successfully eliminated only if the phase function is well sampled. Accordingly, zeroes were appended to the sampled seismogram data vector to make a total length of 1024 points. Because of the nonlinear operations of logarithm, absolute value, and arctangent, harmonics are introduced into $\hat{R}(z)$. As a consequence, $\hat{R}(z)$ is undersampled when $z=e^{j\pi k/N}$, $K=0, 1, \dots, N-1$ as in FFT. Therefore, the procedure of appending zeroes also helps in reducing aliasing in the calculation of the complex cepstrum. Another modification to the data that helps in reducing aliasing is w^t weighting. By selecting an appropriate value of w , it can be insured that the ground impulse response is minimum phase. Moreover, its poles can be moved further inward towards the origin and away from the unit circle on which the z transform is evaluated. This smooths the rapid fluctuations in $\hat{R}(z)$ due to the impulse response, and, as a consequence, the

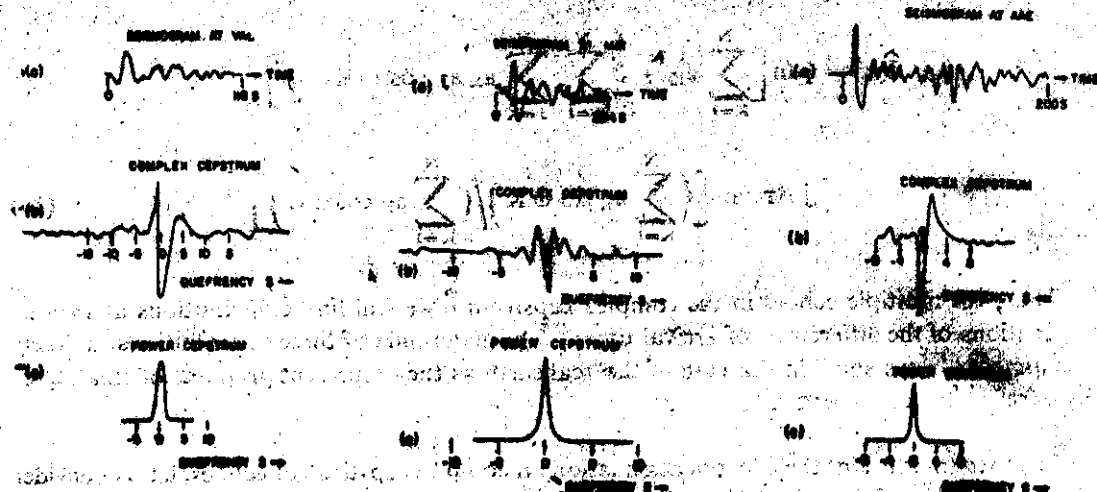


Fig. 1. The seismograms, complex ceptra and power spectra at MAT, AAE and VAL.

higher quenfrequencies and their harmonics in \hat{r} , are attenuated (Stora et al., 1974). The weighting was done in the present analysis with $w = 0.96$.

The complex cepstra obtained in this way are shown in Figure 1. The presence of substantial contributions along the negative quenfrequency axis shows that the source is composed of maximum phase components as well. The form of the complex cepstrum is relatively simple although it differs from station to station. Most of the contribution is concentrated in a ± 5 sec quenfrequency window centered at the origin.

The power cepstra, shown in Figure 1, display a single single peak at the scale in all three cases. This observation also implies that there is no simple echo with significant amplitude present in the seismograms. Normally, the crust introduces complexities in the recorded signal from shallow earthquakes. Viewing the phenomenon of crustal diffraction in terms of rays, these complexities are caused by phases such as pP, pS, sP, sS, etc. These phases may be expected to contribute secondary peaks in the power spectrum. However, for some specific geometries and station locations, the complexities caused by the influence of the direct and the phases reflected from the free surface may be considerably attenuated or absent in the radiation pattern. For the case of the Koyra earthquake the relative theoretical amplitudes for the direct ray and the uppermost ray which forms the pP or sS phases, respectively, are MAT: (1.0; 0.04), AAE: (0.01; 1.0), and VAL: (0.05; 1.0). These values have been calculated for 1 fault plane solution: $\theta = 217^\circ$, $\delta = 27^\circ$, $\lambda = 17^\circ/\text{sec}$ and $t_{\text{min}} = 1.007$. Thus, the information at the above stations would be expected to show dominant direct waves for the P and S waves. Indeed, the wave forms for the Koyra earthquake, shown in Figure 1, appear to be quite free from interference at least for the first 20 sec. Additionally, the observed agreement in the form of the spectra of the source time function and the ground motion response (e.g., equation (12)). If the source time function cepstrum, \hat{r} , has a dominant contribution as compared to \hat{s} , the factor that scales the amplitude of the echo, then the contribution of the

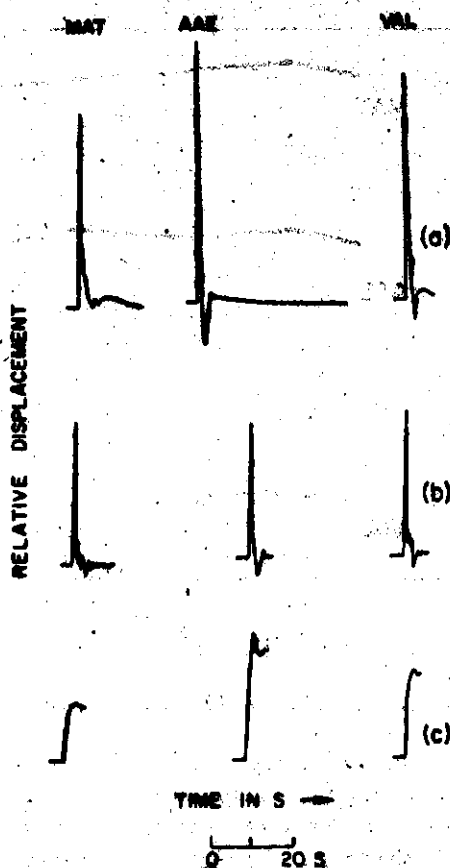


Fig. 2. (a) The recovered ground displacement time functions; (b) the recovered far field (FF) source displacement time functions; and (c) the time integral of (b) approximating near field (NF) source displacement time functions.

echo will not be noticeable in the linear graphs used to represent the cepstra. Similarly, the amplitudes of the other contributions due to the echo die off rapidly as $\alpha < 1$ and will not show up. It would be appropriate to use semilogarithmic plots if the detection of echoes is desired. The above factors together have contributed in producing smooth power cepstra without secondary peaks in the present study.

The fact that the power spectra are very similar in shape in all three cases whereas the complex cepstra are not suggests that the phase content for each seismogram is different. These differences may in part be due to the effects of the transmission path difference and possibly also to the presence of noise in the seismograms (Clayton and Wiggins, 1970). However, even in the presence of noise, up to a signal-to-noise ratio of ten, wavelet estimation can be done satisfactorily (Burgess, 1975). This condition is satisfied for the seismograms recorded at VAL and AAE and nearly so at MAT.

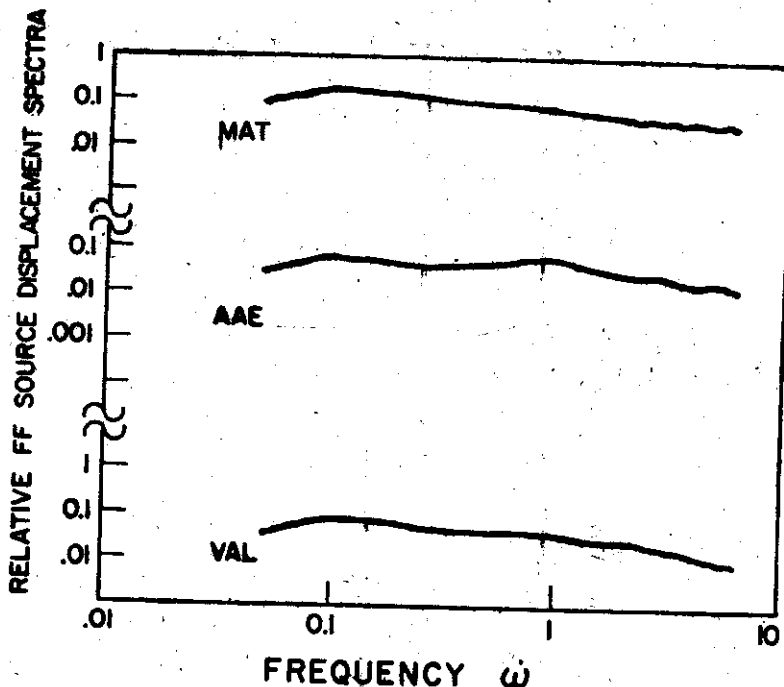


Fig. 3. The amplitude spectra corresponding to FF source displacement time functions of Fig. 2(b).

The next step in our procedure is linear filtering the complex cepstrum to separate the earthquake source time function and the transmission response. The separation criterion for a source wavelet is that its contributions to the complex cepstrum are confined to the neighborhood of zero quefrency. Furthermore, the energy in the complex cepstrum of a wavelet is concentrated in a relatively shorter quefrency (time) duration around the origin, as compared to the time duration of the wavelet (Butkus, 1975; Ulrych, 1971). Therefore, in the filtering process, retaining complex cepstrum contributions in a quefrency window equal to the expected time duration of the source would serve as a safe threshold for recovering the source function. A suitable window length for best results can be obtained by trial and error.

Since the Koyna earthquake was a moderate sized event, we expect the source time function to be less than 4 sec in duration. This assumption is supported by the fault dimension ($r_p \sim 18$ km) and rupture velocity (~ 3 km/sec) estimated for this event (Singh et al., 1975; Khattri et al., 1977). Three filter windows were accordingly tailored to retain all the contributions for quefrencies less than or equal to 4 sec, 8 sec, and 16 sec. The inverse process was then applied to the filtered cepstrum. The resulting signals were unweighted and deconvolved for the instrument response using the transfer function relation given by Hagiwara (1958). The results for the 8 and 16 sec windows were found to be unsatisfactory. The source pulses obtained were of unrealistically long duration. The most satisfactory source time functions were obtained for the 4 sec window and are shown in Figure 2a. The ground displacement time functions show a sharp impulsive wave form with a slight overshoot towards the tail of the signal. The main movement is completed within approximately 3 sec. These wave forms are remarkably similar in shape. From the apparent differences in the complex cepstra, one

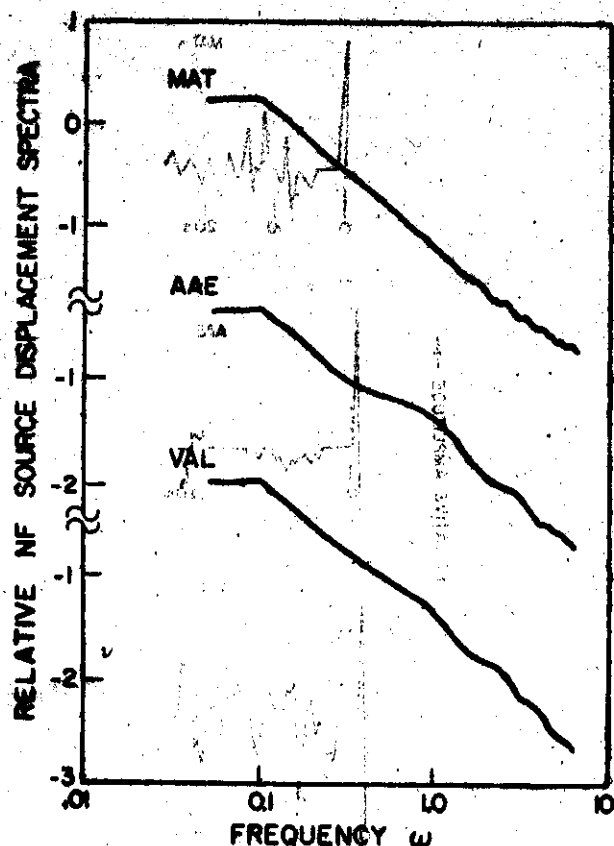


Fig. 4. The amplitude spectra corresponding to PWF source displacement time functions of Fig. 2(c).

would have expected to have recovered substantially different source time functions. However, the complex cepstra are quite similar to each other very near the origin. We therefore infer that our original premise concerning the contributions of the source time function being concentrated near the origin in the quefrency domain is valid.

In order to obtain the signal at the source, we must compensate for the increasing attenuation along the transmission path. The energy loss can be represented by

$$\Delta(\omega) = \exp\left(-\frac{U}{Q} \cdot \frac{\pi}{\lambda} \cdot \frac{d}{U} \cdot Q^2 \cdot \text{erfc}\left(\frac{Q^2 d}{2}\right)\right)$$

where U is the group velocity, d the distance along the ray path and Q the quality factor. For a constant average Q model, the above expression takes the simple form given by

$$\Delta(\omega) = \exp\left(-\frac{U}{Q} \cdot \frac{\pi}{\lambda} \cdot \frac{d}{U} \cdot Q^2 \cdot \text{erfc}\left(\frac{Q^2 d}{2}\right)\right)$$

where $t^* = T/2Q$, in which T is the traveltime, t^* is approximately stationary in the range under study here. The values of t^* were taken to be 0.5 and 2.0 for P and S waves,

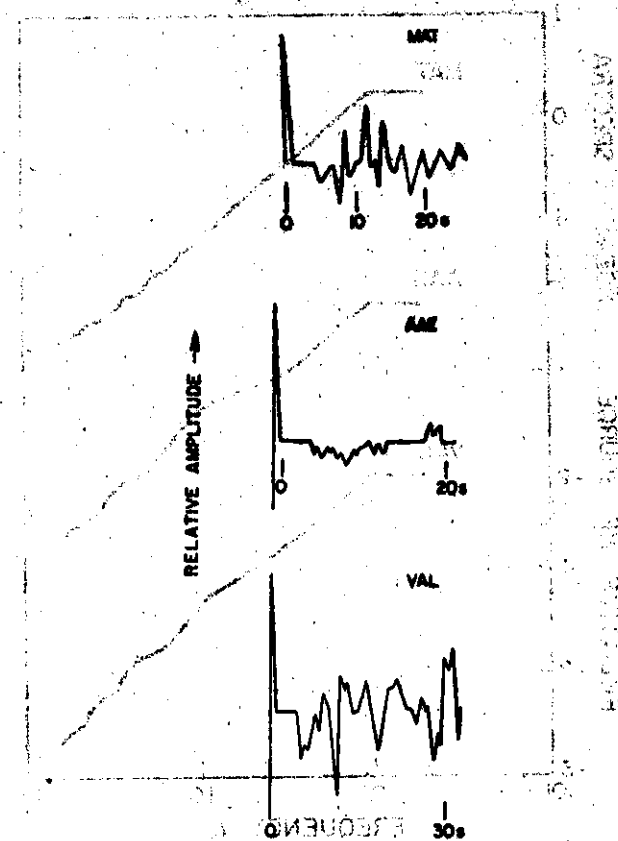


Fig. 5. The recovered ground transmission impulse responses corresponding to the three recording stations used in the study.

respectively (Frasier and Filson, 1972; Helmberger, 1973). The ground displacement pulses projected to the source are shown in Figure 2b. The wave forms have become somewhat sharper. However, a high frequency jitter has appeared towards their tails and the overshoot persists. These wave forms represent the far field time history of the displacement radiation. A common feature of the far field (FF) source time functions is that the onset (first swing) is very sharp. The return swing is equally quick up to about half way down. Thereafter, the backswing rate slows down considerably. The overshoot swing is also rather slow. The FF source time histories are quite similar in shape, with the small differences noticeable towards the tails of the pulse, possibly due to source propagation effects.

Figure 2c illustrates the time integrals of the FF source displacement time functions. These may be considered, to a first approximation, as representatives of the near field (NF) average source displacement time functions. The displacement starts off sharply, slows down somewhat towards the completion of the swing, and shows a small extent of overshoot and backswing.

The phenomenon of observing overshoots in shallow earthquakes was considered improbable by Burridge (1969) on account of friction on the fault surface. However, Bundick and Helmberger (1974) have observed a similar phenomenon for three deep focus earthquakes and offer three possible mechanisms that can produce this feature: (1) slipping on the fault to reduce friction; (2) motion on the surface of the down-going slab; and (3) a coupled set of motions on a pair of fault surfaces. A fourth possible cause can be the elastic overshoot due to the momentum of the slipping opposite sides of the fault surface, which can give rise to elastodynamic radiations seen as backswing.

The amplitude spectra corresponding to the FF and NF source time functions are shown in Figures 3 and 4. The spectra for all the stations are remarkably similar in shape. On a log-log plot the FF spectra decay roughly as ω^{-1} towards higher frequencies, a result which was also obtained by Khattri et al. (1977) using a different approach. We also observe a weak peak in the spectra at $\omega \sim 0.1$. Some theoretical models (e.g., Haskell, 1966; Archambault, 1968) predict the presence of such peaks in the source spectrum. The NF amplitude spectra exhibit a $\sim \omega^{-1.5}$ decay with increasing frequency in the range under consideration. The corner predicted in the seismic source spectrum (e.g., Brune, 1970) is not well developed in the FF source spectra (Figure 3). This may be the consequence of the filtering process which may have to some extent smoothed the spectra. Khattri et al. (1977) obtained corners at frequencies (ω) 0.56 for vertical, 1.0 for NS P wave at AAE, and 0.4 for S wave at VAL. One may interpret corners at $\omega \sim 1.0$ for both AAE and VAL in the present study. The above estimates are in fair agreement with those of Khattri et al., particularly in view of the uncertainty involved in the estimation of corner frequencies (Hanks and Wyss, 1972).

The transmission impulse responses obtained by retaining only the minimum phase high quefrency components in the inversion process are shown in Figure 5. The information in the first few seconds is completely lost. It is included in the source waves as noise. This noise should be small as acoustic impedances in sedimentary layers would be relatively small and contribute only weak reverberations. These transmission responses include the effects of source crust, receiver crust, and mantle propagation convolved together.

Conclusions

Currently, in a number of investigations, various parameters such as the corner frequency or the peak frequency of the far field source spectrum have been used to infer source parameters, typically: the fault dimensions, rupture velocity, and stress drop. However, the interpretation of these spectral parameters depends critically on the source time function model used to represent the earthquake source (e.g., Savage, 1972). Furthermore, techniques based solely on amplitude spectra neglect an important source of information, that of phase. It appears necessary to estimate accurately the source time histories of earthquakes in order to distinguish between competing models. Accurate source time histories will also provide better estimates of the fine structure of the earth along the transmission path by means of deconvolution procedures. LOG-EXP processing offers a method for accomplishing the above objectives, as demonstrated in this preliminary analysis. The source time functions for the Koyna earthquake obtained from all three recordings show an impulsive wave form with a small overshoot. The pulse decay slows down somewhat towards the end of the first half cycle. The next two half

cycles, of considerably smaller amplitude, are also broad as compared to the initial cycle. These results suggest that for the Koyra earthquake, most of the energy was released in about 3 sec. We note that Langston (1970) used a triangular pulse of 5.5 ± 1.3 sec time duration to obtain synthetic seismograms comparable to those observed. The source time pulse duration obtained in the present study is ~ 4 sec.

Acknowledgment

Many valuable comments were made by Drs. Carl Kisslinger, Charles Archambeau, and Stuart Wier, who kindly read the manuscript critically. We are grateful to Ms. M. Lund for preparing the manuscript and Mr. R. McDonald for his excellent drafting of the figures. The computer work was supported by the Department of Earth Sciences, Roorkee University, the Oil and Natural Gas Commission, Dehradun, and the Cooperative Institute for Research in Environmental Sciences, University of Colorado/NOAA.

References

- Archambeau, C.B., General theory of elastodynamic source field, *Rev. Geophys.*, 6, 241-288, 1968.
- Archambeau, C.B., and J.B. Minster, Dynamics in prestressed media with moving phase boundaries: A continuum theory of failure in solids, *Geophys. J.*, in press, 1977.
- Ben-Monahem, and S.J. Singh, Computation of models of elastic dislocations in the earth, in *Methods of Computational Physics*, Academic Press, New York, 12, 299-375, 1972.
- Bogart, B.P., M.J.R. Healy, and J.W. Tukey, The quasirecency analysis of time series for echoes: Cepstrum, pseudo-autocovariance, cross-cepstrum, and seismic cracking, *Proc. Symposium on Time Series Analysis*, ed. M. Rosenblatt, Wiley and Sons, Inc., New York, 205-243, 1963.
- Bruno, J., Tectonic stress and the spectra of seismic shear waves from earthquakes, *J. Geophys. Res.*, 75, 4997-5009, 1970.
- Burdick, L.J., and D.V. Helmberger, Time functions appropriate for deep earthquakes, *Bull. Seism. Soc. Amer.*, 64, 1419-1428, 1974.
- Burridge, R., The numerical solution of certain integral equations with non-integrable kernels arising in theory of crack propagation and elastic wave diffraction, *Phil. Trans. Roy. Soc. (London)*, Ser. A., 265, 353-381, 1969.
- Butkus, B., Homomorphic filtering-theory and practice, *Geophys. Prospecting*, 23, 712-748, 1975.
- Clayton, R.W., and R.A. Wiggins, Source shape estimation and deconvolution of teleseismic body waves, *Geophys. J. Roy. Astr. Soc.*, 47, 151-177, 1976.
- Dziewonski, A.M., and F. Gilbert, Temporal variation of the seismic moment tensor and the evidence of precursive compression for two deep earthquakes, *Nature*, 247, 185-188, 1974.

- Frasier, C.W., and J.A. Filson, A direct measurement of the earth's short-period attenuation along a teleseismic ray path, *J. Geophys. Res.*, **77**, 3782-3787, 1972.
- Hagiwara, T., A note on the theory of the electromagnetic seismograph, *Bull. Earthquake Res. Inst., Tokyo Univ.*, **36**, 139-164, 1958.
- Hanks, T.C., and M. Wyss, The use of body waves spectra in the determination of seismic parameters, *Bull. Seism. Soc. Amer.*, **63**, 633-646, 1972.
- Haskell, N.A., Total energy and energy spectral density of elastic wave radiation from propagating faults. Part II. A statistical source model, *Bull. Seism. Soc. Amer.*, **56**, 125-140, 1966.
- Helmburger, D.V., On the structure of the low velocity zone, *Geophys. J.*, **34**, 251-263, 1973.
- Kemerait, R.C., and D.G. Childers, Signal detection and extraction by cepstrum techniques, *IEEE Trans. on Info. Theo.* IT-18 (6), 745-759, 1972.
- Khattri, K.N., A.K. Saxena, and H. Sinhal, Determination of seismic source parameters for the 1967 earthquake in Koyna Dam region, India, using body wave spectra, *Proc. 6th World Conference on Earthquake Engineering*, New Delhi, India, Vol. 2, 308-316, 1977.
- Langston, C.A., A body wave inversion of the Koyna, India, earthquake of December 10 1967, and some implications for body wave focal mechanisms, *J. Geophys. Res.*, **81**, 2517-2529, 1976.
- Lee, W.H.K., and C.B. Raleigh, Fault plane solution of the Koyna (India) earthquake, *Nature*, **233**, 172-173, 1969.
- Molnar, P., B.E. Tucker, and J.N. Brune, Corner frequencies of P and S waves and models of earthquake sources, *Bull. Seism. Soc. Amer.*, **63**, 2091, 1968.
- Oppenheim, A.V., R.W. Schafer, and T.G. Stockham, Jr., Non-linear filtering of multiplied and convolved signals, *Proc. IEEE*, **56**, 1264-1291, 1968.
- Robinson, E.A., *Statistical communication and detection*, Hafner Publishing Co., New York, 1967.
- Savage, J.C., Relation of corner frequency to fault dimensions, *J. Geophys. Res.*, **77**, 3788-3795, 1972.
- Schafer, R.W., Echo removal by discrete generalized linear filtering, Research Lab. of Electronics, M.I.T., Technical Report 466, 1969.
- Singh, D.D., B.K. Rastogi, and H.K. Gupta, Surface wave data and source parameters of Koyna earthquake of Dec. 10, 1967, *Bull. Seism. Soc. Amer.*, **65**, 711-731, 1975.
- Stoffa, P.L., P. Bhul, and G.M. Bryan, The application of homomorphic deconvolution to

- shallow-water marine seismology—Part I: Models. *Geophysics*, 39, 401–416, 1974.
- Ulrych, T.J., Application of homomorphic deconvolution to seismology. *Geophysics*, 36, 630–660, 1971.
- Ulrych, T.J., O.G. Jensen, R.M. Ellis, and P.G. Somerville, Homomorphic deconvolution of some teleseismic events. *Bull. Seism. Soc. Amer.*, 62, 1269–1281, 1972.
- Wyss, M., and P. Molnar, Source parameters of intermediate and deep focus earthquakes in the Tonga Arc. *Phys. Earth Planet. Inter.*, 6, 279–292, 1974.